Receiver Beam Characterization for the SMA

M. T. Chen[a], C. -Y. E. Tong[b], R. Blundell[b], D. C. Papa[b], and S. Paine[b]

[a]Institute of Astronomy and Astrophysics, Academia Sinica
Nankang P.O. Box 1-87, Taipei, Taiwan 115

[b]Harvard-Smithsonian Center for Astrophysics
Cambridge, Ma 02138, USA

ABSTRACT

This paper describes the measurements and subsequent data analysis of the signal beam of the receiver system of the Submillimeter Array (SMA). To measure the receiver beam patterns, a 2-axis planar scanning stage is mounted onto the top of the receiver assembly. Scanning in a plane orthogonal to the optical path, the near-field measuring system maps out both the amplitude and phase at frequencies of 242 and 265 GHz. By analyzing the measured patterns we can inspect the alignment of the individual receiver, and the optical assembly common to all frequency bands. The data also allows us to determine how the receiver beam matches to the beam waveguide that feeds the primary and secondary mirrors of the telescope. We shall describe the beam measurement set-up related techniques. The measured beam patterns of two different receivers, covering frequency bands of 176-256 and 250-350 GHz, respectively, will be presented, as well as the analysis of these data. We believe that this is the first time such rigorous full vectorial radio alignment techniques have been applied to millimeter or sub-millimeter receiving system of radio astronomy.

Keywords: The Submillimeter Array, beam pattern, radio alignment, near field measurement

1. INTRODUCTION

The Submillimeter Array (SMA), currently under construction by the Smithsonian Astrophysical Observatory (SAO) and the Institute of Astronomy and Astrophysics of Academia Sinica in Taiwan, will function as a fully automated radio interferometer of eight 6-m antennas. Fixed-tuned receivers incorporating superconductor-insulator-superconductor (SIS) mixers are being developed to cover the major submillimeter atmospheric windows from 176 GHz to 900 GHz.

The design and development of the receiver system, including the SIS mixers[1,2,3,4,5] and the beam waveguide optics[6] system, have been reported previously. The first prototype SMA receiver system equipped with two SIS receiving modules has been built in the Receiver Lab of the SAO. It covers two frequency channels of 176-256 GHz and 250-350 GHz. As part of the receiver system integration effort, the beam patterns of the receiver at each frequency channel are *measured in-situ* after the receiver is completely assembled. The measured patterns are compared to the designed patterns to determine whether the receiver feeds the beam waveguide of the telescope as designed.

Another motivation of this near-field measurement exercise is to examine the alignment of the receiver optics. Millimeter and sub-millimeter wavelength systems often involve quasi-optical components such as wire grids, dielectric lenses, and beam-splitters. In the case of a cryogenic receiver, an optically opaque vacuum window is utilized to block off thermal radiation. It becomes impractical to carry out an optical alignment procedure in such a receiver system. This problem can be solved by examining the beam profile of receiver at an appropriate position in the signal path. Misalignment of individual quasi-optical components eventually results in a distorted beam pattern. With further numerical analysis, one can obtain information on how to correct the problem in a complex receiver system.

Further author information –
MTC (correspondence): mchen@biaa.sinica.edu.tw

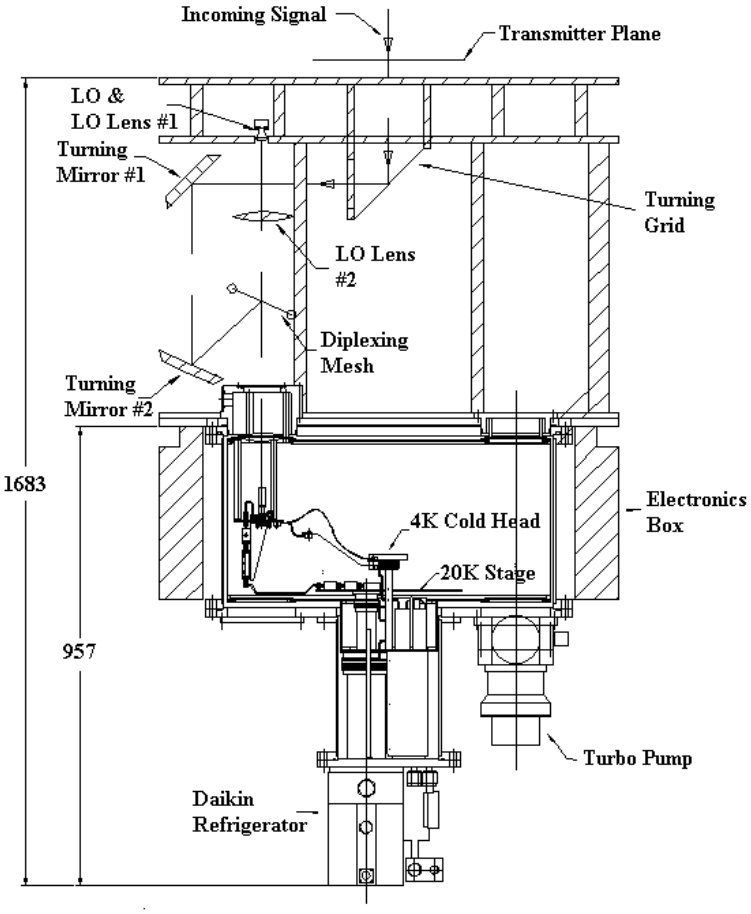

FIGURE 1: Signal path schematic of the SMA receiver system. Dimensions are in mm.

The measured beam profiles are processed numerically by a near-field transform based on a vector Kirchhoff integral formalism[7]. By analyzing the transformed field pattern at different locations, we are able to inspect the mechanical alignment of the receiver system. This approach provides a means to improve the alignment. The development of this new radio alignment technique is described.

This paper is organized as follows: It first shows the physical layout of the receiver system to show the signal path in the receiver. It is followed by a discussion on the beam measurement assembly. The alignment accuracy of the setup is next discussed. Then, the measured results are presented, along with the discussion on the receiver performance and its optics alignment.

2. THE RECEIVER SYSTEM

A schematic of the SMA receiver system is shown in Fig. 1. In this figure we indicate the signal path and the key optical components, as well as the cryostat that contains the SIS receiver module and the IF amplifier chain. The incoming signal beam enters the receiver from a top opening and is separated into 2 orthogonally polarized beams by a 45-degree wire grid. The grid is made of 20 um tungsten wires wound at 60 um pitch. It is integrated into a rotating holder that can be horizontally

rotated to select different receiver channels. The beam reflected off the grid is used to couple to the lower frequency mixers (176-256 GHz and 250-350 GHz) while the transmitted beam is designated as the high frequency component. The optics for the higher frequency mixers is being designed.

The lower frequency signal beam then enters an optical sub-assembly for each receiver module. This assembly contains two turning mirrors for the incoming signal, a Teflon lens for focusing local oscillator signal, and a fine mesh for signal and LO injection. The LO chain is located in the upper part of the optics assembly, and is not shown in the schematic. After reflecting off the diplexing mesh, signal beam enters the cryostat through a vacuum window on the top of the receiver module. The material used for the window is a 0.5mm thick Teflon sheet. Inside the dewar, signal is re-focused by a Teflon lens mounted at the 80K plates of the module. This lens also functions as an infra-red shield to block off thermal radiation. Through a corrugated feed horn, the focused beam is coupled to an SIS mixer inside a mixer block. The mixer block with feed horn is mounted on the 4 K stage of the module. A detail schematic of the module is shown in Fig. 2. We refer to Ref. 6 for a detail configuration on the SMA optics design.

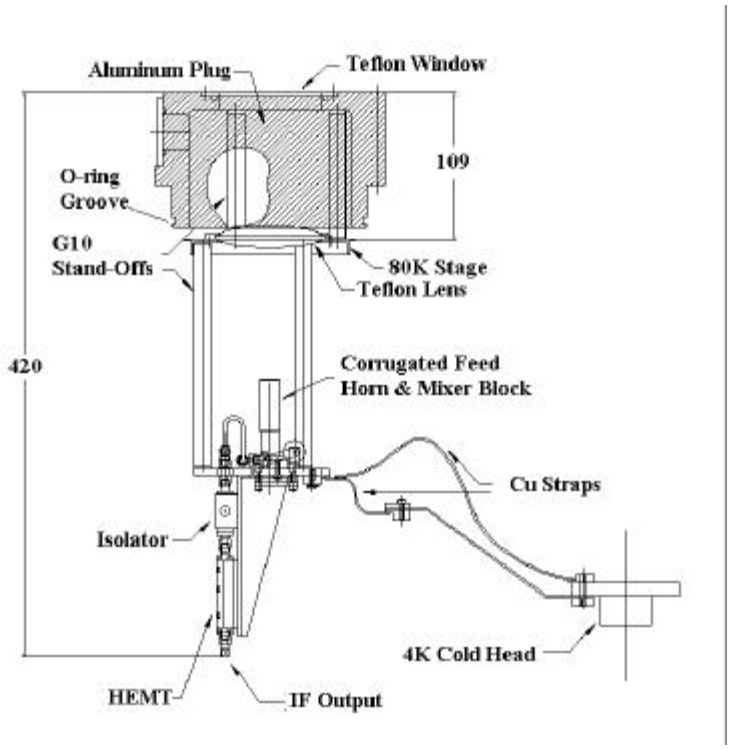

FIGURE 2. Insert schematics of the 216 GHz channel receiver. Dimensions are in millimeter.

The receiver module is designed as a plug-in insert on top of the cryostat. In terms of temperature, it is composed of three main parts, separated by stand-offs made of glass-fiber tubes. The room temperature part is a circular plug made of aluminum, with its center bored out for signal entrance. The 80K stage is mainly a lens holder, and it makes contact with the 80 K radiation shield via a ring of BeCu spring fingers. The 4K stage is connected to the cold head through flexible pure Cu straps. On the 4K stage are the SIS mixer block, followed by an isolator, and a HEMT amplifier (made by NRAO). The HEMT operates at 5 GHz with a 2 GHz bandwidth. The IF is further amplified at the 20 K cooling stage of the cryostat before exiting the dewar.

3. SCANNER SETUP

To map out the receiver beam pattern, we set up an XY translation stage on top of the receiver system The XY plane is

set to be perpendicular to the signal path. A high-frequency transmitter mounted on the translation stage is used as a signal source. A block diagram of the measurement setup is presented in Fig.3. The signal is generated by a frequency multiplier, which is pumped by a phased-locked Gunn oscillator. The probe of the transmitter is a WR-3 open waveguide with its front wall chamfered to reduce the cross-sectional area. The total radiated power is in the order of micro-Watts. The master reference signal for the entire system is the 10 MHz internal reference of a signal synthesizer. The output of the synthesizer at around 15 GHz is used to lock the Gunn oscillators of the LO chain and the transmitter. The receiver IF output at around 5 GHz is down-converted to 80 MHz and measured against a reference signal by a vector voltmeter.

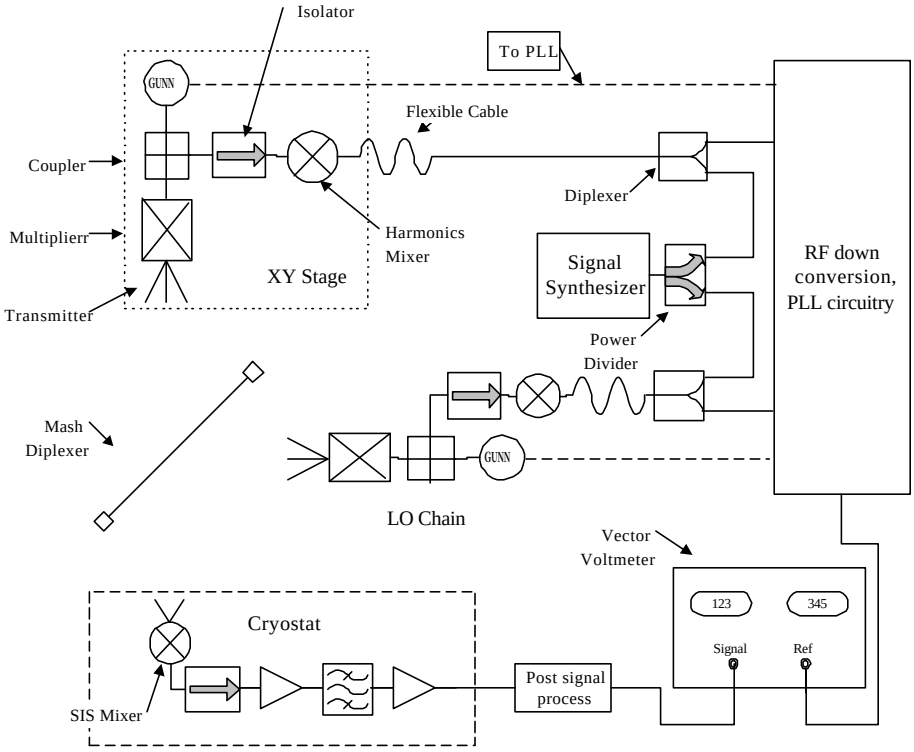

FIGURE 3. Block diagram of the beam measurement setup.

In order to test two different receiver inserts with the same setup, the transmitter is tuned to operate at 242GHz for the 176-256 GHz (216) band, and 265 GHz for the 250-350 GHz (300) band. A dynamic range of more than 50 dB, and instantaneous phase fluctuation less than 5 degree are achieved with the current setup. The scan area is typically of 120 mm X 120 mm. The scanning time is mainly limited by the speed of the stepper motor. In a typical scan with scanning point 1.5 mm apart on a square mesh, total scan time is around 100 minutes. No probe correction has been applied to the measured data because the beams are essentially paraxial.

Special precautions have been taken to ensure that the scan plane is normal to the optical axis of the receiver assembly. We have measured that the scan plane is parallel to the top plate of the receiver assembly to within 50 um over a distance of 150 mm. Long-term phase drift caused by ambient temperature fluctuations can also introduce artificial pointing error in our measurement. To reduce such effects, we adopt a modified raster scanning pattern. A simple illustration of the pattern is shown in Fig. 4. At the center of each row scan, the probe moves to the center of the scan plane to register a set of data. After a scan, each row is corrected with the center registration. The corrected phase fluctuation is fairly low, estimated to be about 3 degrees RMS at 240 GHz, which is about 10 um, over a distance of 150 mm. This error is taken as an additional alignment error. Combined with the positioning error of the probe, we have a total misalignment budget of 60 um over 150 mm, equivalent to a maximum misalignment of 1.4 arc minutes.

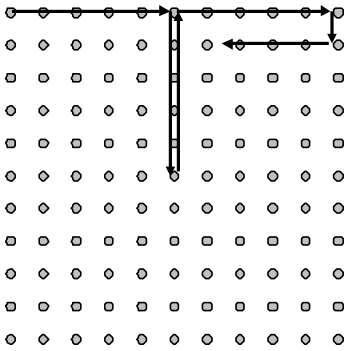

FIGURE 4. Illustration of the probe's movement. At the center of each row scan, the probe moves back to the center of the scan plane to register power and phase drifts.

4. RESULTS AND DISCUSSION

Initial system alignment is performed optically with lasers. Once the optical alignment is done, different scans are carried out for each insert under test. Shown in Fig. 5 are the measured beam patterns for the 216 GHz and 300 GHz inserts measured at 242 GHz and 265 GHz, respectively. The data shows that center of the beam at the scan plane is not at the optical axis of the receiver assembly. By fitting the pattern to a quadratic function, we can find the center of the contours of the measured beam. Table 1 shows the fitting result.

TABLE 1. Contour center from quadratic fitting		
	216 GHz	300 GHz
Power	(6, 8)	(1, -4)
Phase	(-3, -3)	(2, 0)

We have compared the measured beam pattern to the theoretical designed field. A complex overlap summation is performed by taking the complex multiplication of the fields at each scan point and sum over the entire scan plane. Each field is first normalized with its total power in the entire scan plane. The result is an indication that how well the measured beam matches to its design. The overlap summation yields magnitudes of 0.93 for the 242GHz beam, and 0.95 for the 265 GHz. It is evident that the 216 GHz insert has a severe alignment problem, while the 300 GHz one seems to be reasonably aligned for the first time. Thorough examination on each component is currently under way. On the other hand, we are also pursuing a method to inspect the effect on the insert structure due to cooling down.

As an aide to pinpoint the alignment problem, we are developing a novel technique that is an extension from our field modeling method. In this method, we place a scatterer at a known position along the signal path. Scatterer, such as a cross-wire, is arranged such that it can define the designated beam center. The resultant beam pattern is then measured, and taken as an initial field for a near-field transformation using a Kirchhoff integral[7],

$$\vec{E}(\vec{r}) = \frac{1}{2p}\int_S \frac{e^{ikR}}{R^2}\left[jk - \frac{1}{R}\right]\cdot \vec{R}\times\left[\hat{z}\times \vec{E}(\vec{r}_0)\right]\cdot dS \qquad (1)$$

where k is the propagation constant, $\hat{z}$ is the unit normal vector of the plane defined by $\vec{r}_0$ and $\vec{R} = \vec{r} - \vec{r}_0$. Using the above formalism, we have developed a computer code to calculate the electric field on a target plane of interest (scatter plane) from

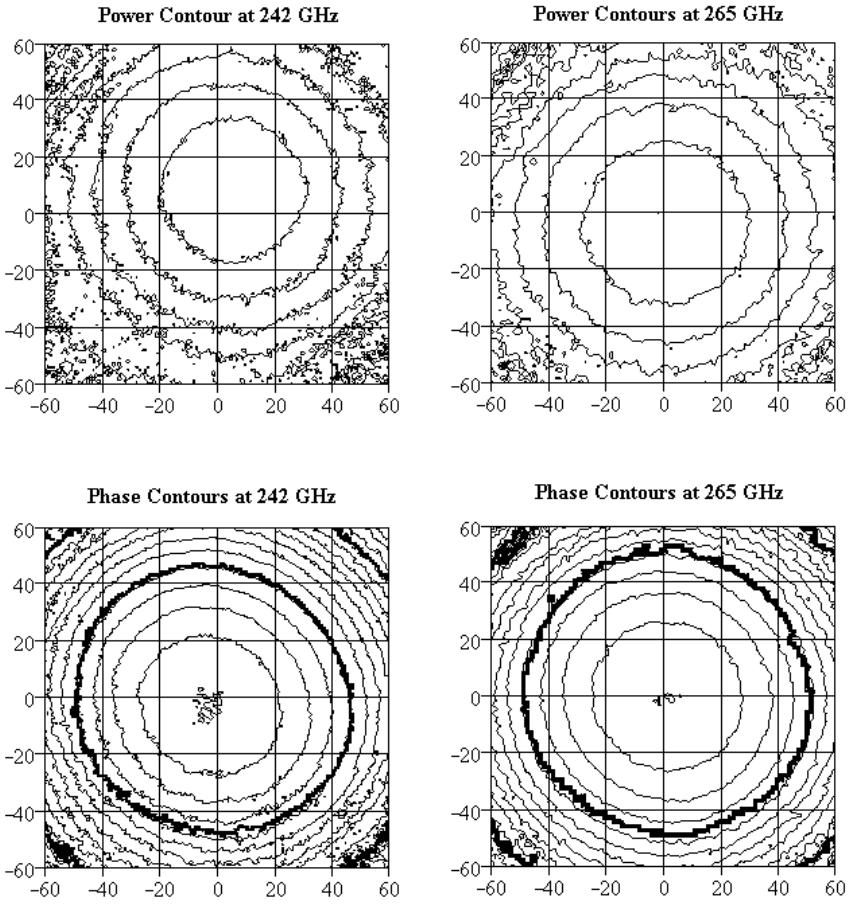

FIGURE 5. Measured beam patterns of the MSA receiver system. The 216 GHz band is measured at 242 GHz, and the 300 GHz band at 265 GHz. The power contours are every 5dB descending from the center, while the phases are 50 degrees. The X- and Y-axes are in millimeters.

an initial plane with known field distribution (measured pattern). This approach allows us to re-construct the signal beam at the scatterer. By comparing the transformed beam with and without the scatterer, we directly inspect if the receiver structure or the optical components are aligned between the scatterer and the scanner.

Preliminary scans utilizing this technique have been carried out for the 216 GHz Insert. Figure 7 shows the differential power pattern from the measurements. The scatterer is a cross-wire with wire thickness of 1.2 mm. The scatter plane is about 370 mm from the scanner, a position between the turning grid and the upper turning mirror. From the pattern we can clearly see the center of the cross, which is about 1 mm off the center. The deviation may be accumulated from the measurement error, especially from placement of the scatter. However, the obvious conclusion is that the rotating grid should not be the problem that causes the misalignment of the insert.

The advantage of this technique is to provide an *in situ* way to inspect individual component in a complex, radio-wavelength receiving system. With careful design, one can perform a precise system alignment on those radio-transparent, but optical-opaque components. It provides a "zooming" effect similar to optical means. There are some limitations. To have an effective zooming effect, the size of the scatterer, the scan area, and scan resolution, and the distance between the scatter the scanner have to be decided carefully. This part of the work is still underway. A more complete result

will be reported in the future.

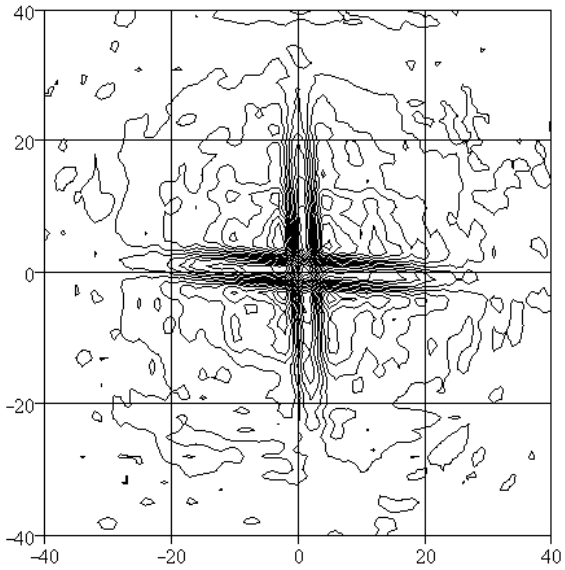

FIGURE 6. Differential power contours of a scattering pattern induce by a cross wire in the signal path.

5. SUMMARY

The SMA receiver system is a state-of-the-art equipment aiming at exploring the Universe in the sub-millimeter wavelength for the next century astronomy. From its design, construction, testing, and finally to the current status, it has span many years of team effort from many talented researchers and engineers. In this paper, we have focused on report the receiver 's working status to the moment. The beam patterns for the lower two designated frequency band have been measured and analyzed. From the measurement, we have showed that further alignment need to be done. It has also shown that it is necessary to perform detailed beam measurements to inspect system alignment for the SMA receiver optics, which involves mirrors, quasi-optical devices, and cryogenics components.

We have also demonstrated a novel alignment technique suitable for the SMA receiver system, and system alike. For the case where optical mean is not feasible, this techniques is useful for aligning RF components in a complex system often seen in a beam waveguide telescopes. More work in underway to explore this method for more usefulness.

6. ACKNOWLEDGMENT

The authors would like to thank Mr. Mike Smith for his superior technical assistance in aligning the receiver optics. Funding for MTC is supported in part by the National Science Council of Taiwan under a grant NSC-87-2213-E-001-028.

7. REFERENCES

[1.] R. Blundell, C.-Y. E. Tong, D. C. Papa, R. L. Leombruno, X. Zhang, S. Paine, J. A. Stern, H. G. LeDuc, and B. Bumble, "A Wideband Fixed-Tuned SIS Receiver for 200-GHz Operation," IEEE Trans. Microwave Theory Tech., **MTT-43**, pp.933-937, 1995.

[2] R. Blundell, C.-Y. E. Tong, J. W. Barrett, J. Kawamura, R. L. Loembruno, S. Paine, D. C. Papa, X. Zhang, J. A. Stern, H. G. LeDuc, and B. Bumble, "A Fixed Tuned Low Noise SIS Receiver for the 450 GHz Frequency Band," Proc.6th Int. Symp. Space Terahertz Tech. 1995.

[3] C.-Y. E. Tong, R. Blundell, S. Paine, D. C. Papa, J. Kawamura, X. Zhang, J. A. Stern, and H.G. LeDuc, "Design and Characterization of a 250-350 GHz Fixed-Tuned Superconductor-Insulator-Superconductor Receiver," IEEE Trans. Microwave Theory Tech. **MTT-44,** pp. 1548-1556, 1996.

[4] C.-Y. E. Tong, R. Blundell, D. C. Papa, J. W. Barrett, S. Paine, X. Zhang, J. A.Stern, and H. G. LeDuc, "A Fixed Tuned Low Noise SIS Receiver for the 600 GHz Frequency Band," Proc. 6th Int. Symp. Space Terahertz Tech. 1995.

[5] M. T. Chen, C. E. Tong, S. Paine, and R. Blundell, "Characterization of Corrugated Feed Horns at 216 and 300 GHz", International Journal of Infrared and Millimeter Waves, Vol. 18, No.9, pp. 1697-1710, 1997.

[6] S. Paine, D. C. Papa, R. L. Leombruno, X. Zhang, and R. Blundell, "Beam Waveguide and Receiver Optics for the SMA," Proc. 5th Int. Symp. Space Terahertz Tech. 811-823, 1994.

[7] Thorkild B. Hansen and Arthur D. Yaghjian, "Planar Near-Field Scanning in the Time Domain, Part 1: Formulation," IEEE Tans. Antennas Propagat., AP-42, No.9, pp. 1280-1291, 1994.